ELSEVIER

International Journal of Solids and Structures 41 (2004) 1435–1451

INTERNATIONAL JOURNAL OF SOLIDS and STRUCTURES

www.elsevier.com/locate/ijsolstr

Stress analysis of an elastic cracked layer bonded to a viscoelastic substrate

C.C. Hsiao [a], C.K. Chao [a,*], R.C. Chang [b]

[a] Department of Mechanical Engineering, National Taiwan University of Science and Technology, 43 Keelung Road, Section 4, Taipei, 106, Taiwan, ROC

[b] Department of Mechanical Engineering, St. John's & St. Mary's Institute of Technology, 499 Tam King Road, Section 4, Tamsui, 251, Taiwan, ROC

Received 7 May 2003; received in revised form 6 October 2003

Abstract

The effect of a viscoelastic substrate on an elastic cracked layer under an in-plane concentrated load is solved and discussed in this study. Based on a correspondence principle, the viscoelastic solution is directly obtained from the corresponding elastic one. The elastic solution in an anisotropic trimaterial is solved as a rapidly convergent series in terms of complex potentials via the successive iterations of the alternating technique in order to satisfy the continuity condition along the interfaces between dissimilar media. This trimaterial solution is then applied to a problem of a thin layer bonded to a half-plane substrate. Using the standard solid model to formulate the viscoelastic constitutive equation, the real-time stress intensity factors can be directly obtained by performing the numerical calculations. The results obtained in this paper are useful in studying the problem with bone defects where a crack is assumed to exist in an elastic body made of the cortical bone that is bonded to a viscoelastic substrate made of the cancellous bone.

Keywords: Viscoelasticity; Bone structure; Layer problem; Crack; Stress intensity factors; Stress analysis

1. Introduction

Prediction of the time-dependent failure behavior of viscoelastic structures has aroused much attention because these components have been widely used in numerous engineering designs in recent years. Thin film and substrates can be treated as important components in many applications including mechanical devices, electronic substrates, medical engineering and building structures. Defects like cracks in these components are inevitable and affect the performance of the system. For example, cracks in the thin film can have a strong adverse effect on the strength of semiconductor materials. When the viscoelastic effects are involved in the analysis, it is well known that there exists a correspondence principle provided that the Laplace transforms of the linear viscoelastic equations are identical to the elastic equations where the constant

* Corresponding author. Fax: +886-2-2737-6460.
E-mail address: ckchao@mail.ntust.edu.tw (C.K. Chao).

0020-7683/$ - see front matter
doi:10.1016/j.ijsolstr.2003.11.007

elastic moduli are replaced by the corresponding transform viscoelastic moduli. However, the real-time solution to the crack-tip field of a dissimilar media is by no means straightforward. Hence, due to the complication of the inverse Laplace transform, most studies have focused on the anti-plane problem in order to simplify the calculation for the real-time response.

The crack problem of dissimilar media in plane elasticity has been studied and collected in the literature. Miller (1989) analyzed the problem of cracks near interfaces between dissimilar anisotropic materials by using the complex variable formulation of Leknitskii (1963). Suo (1990) provided a formal treatment of interfacial crack problems involving singularities embedded in an anisotropic media by using the formalisms derived from Leknitskii (1963), Eshelby et al. (1953), and Stroh (1958). When the problem with multiple layered media is considered, an exact solution satisfying all the interface boundary conditions is impossible to achieve. To treat this complicated problem, the alternating technique is used to look for a series solution by successive approximations, which resembles the method of images in potential theory, in which an infinite number of image singularities are constructed. For example, Chao and Kao (1997) analyzed an isotropic trimaterial under an anti-plane concentrated force through iterations of Möbius transformation. Choi and Earmme (2002a,b) used the alternating technique to analyze the effects of singularities interacting with interfaces in an anisotropic and an isotropic trimaterial.

As to viscoelastic materials, Atkinson and Bourne (1989) applied an integral transform method to study the problem of a semi-infinite crack meeting an interface between dissimilar isotropic viscoelastic materials under anti-plane strain deformation. Ryvkin and Banks-Sills (1993, 1994) determined the mode-II stress intensity factor for a crack propagating steadily between two-bonded viscoelastic infinite strips by using both Maxwell's model and the standard solid model to simulate the viscoelastic behavior. Atkinson and Chen (1996) studied the anti-plane analysis of a crack lying in a viscoelastic layer embedded in a different viscoelastic medium. More recently, Chang (2002) studied the influence of various bonded layers on stress intensity factors of an inclined crack lying in a viscoelastic multi-layered medium under an anti-plane concentrated load. Chang et al. (2001) discussed the effect of a viscoelastic substrate on a cracked body under an in-plane concentrated load.

In this study, we use an alternating technique to solve the in-plane stress intensity factor of a crack lying in an anisotropic elastic thin layer bonded to a viscoelastic substrate. The solution associated with singularities in dissimilar media is derived from that associated with singularities in the corresponding homogeneous medium. With the aid of the dual coordinate transformation, a singular integral equation is solved to obtain the asymptotic solution to a crack with arbitrary orientations. Using the standard solid model to simulate the viscoelastic constitutive equation and applying an inverse Laplace transform by the aid of Mathematica software, the real-time stress intensity factors are determined. Numerical examples of a crack located arbitrarily in a thin layer made of the cortical bone bonded to a viscoelastic substrate made of the cancellous bone are considered and discussed in detail.

2. Basic formulation for two-dimensional anisotropic elasticity

The generalized Hook's law connecting strains ε_m and stresses σ_m for an anisotropic elastic material can be expressed in the following forms (Leknitskii, 1963):

$$\varepsilon_m = s_{mn}\sigma_n \quad (m, n = 1, 2, 3, \ldots, 6), \tag{1}$$

where s_{mn} denotes the second-order compliance tensor. The standard correspondent strains and stresses are

$$\begin{aligned} \{\varepsilon_m\} &= \{\varepsilon_{11}, \varepsilon_{22}, \varepsilon_{33}, 2\varepsilon_{23}, 2\varepsilon_{31}, 2\varepsilon_{12}\}^{\mathrm{T}} \\ \{\sigma_n\} &= \{\sigma_{11}, \sigma_{22}, \sigma_{33}, \sigma_{23}, \sigma_{31}, \sigma_{12}\}^{\mathrm{T}} \end{aligned} \tag{2}$$

where the superscript T denotes the transpose of a matrix. The well-developed two-dimensional anisotropic elastic field can be represented by a stress function involving three stress functions as (Leknitskii, 1963)

$$\boldsymbol{f}(z) = [f_1(z_1), f_2(z_2), f_3(z_3)]^{\mathrm{T}} \tag{3}$$

with the arguments

$$z_\alpha = x_1 + \mu_\alpha x_2, \quad (\alpha = 1, 2, 3) \tag{4}$$

where the elastic eigenvalues $\mu_\alpha (\alpha = 1, 2, 3)$ have to satisfy the sixth-order characteristic equation

$$l_2(\mu) l_4(\mu) - l_3^2(\mu) = 0 \tag{5}$$

with

$$\begin{aligned} l_2(\mu) &= s_{44} - 2s_{45}\mu + s_{55}\mu^2 \\ l_3(\mu) &= -s_{24} + (s_{25} + s_{46})\mu - (s_{14} + s_{56})\mu^2 + s_{15}\mu^3 \\ l_4(\mu) &= s_{22} - 2s_{26}\mu + (2s_{12} + s_{66})\mu^2 - 2s_{16}\mu^3 + s_{11}\mu^4 \end{aligned} \tag{6}$$

The traction and displacement on the x_2-plane of two-dimensional anisotropic elasticity can be written as

$$\begin{aligned} \boldsymbol{t} &= [\sigma_{21}, \sigma_{22}, \sigma_{23}]^{\mathrm{T}} = 2\Re\{L_{ij} f_j'(z_j)\} \\ \boldsymbol{u} &= [u_1, u_2, u_3]^{\mathrm{T}} = 2\Re\{A_{ij} f_j(z_j)\} \end{aligned} \tag{7}$$

where $i = j = 1, 2, 3$ and $\Re$ denotes the real part of the complex function. The 3×3 matrices $\boldsymbol{A}$ and $\boldsymbol{L}$ associated with the elastic constants are defined as (Leknitskii, 1963)

$$\boldsymbol{L} = \{L_{ij}\} = \begin{bmatrix} -\mu_1 & -\mu_2 & -\mu_3\eta_3 \\ 1 & 1 & \eta_3 \\ -\eta_1 & -\eta_2 & -1 \end{bmatrix} \tag{8}$$

$$\boldsymbol{A} = \{A_{ij}\} = \begin{bmatrix} A_{11} & A_{12} & A_{13} \\ A_{21} & A_{22} & A_{23} \\ A_{31} & A_{32} & A_{33} \end{bmatrix} \tag{9}$$

where

$$\begin{aligned} A_{11} &= s_{11}\mu_1^2 + s_{12} - s_{16}\mu_1 + \eta_1(s_{15}\mu_1 - s_{14}) \\ A_{21} &= s_{21}\mu_1 + s_{22}/\mu_1 - s_{26} + \eta_1(s_{25} - s_{24}/\mu_1) \\ A_{31} &= s_{41}\mu_1 + s_{42}/\mu_1 - s_{46} + \eta_1(s_{45} - s_{44}/\mu_1) \\ A_{12} &= s_{11}\mu_2^2 + s_{12} - s_{16}\mu_2 + \eta_2(s_{15}\mu_2 - s_{14}) \\ A_{22} &= s_{21}\mu_2 + s_{22}/\mu_2 - s_{26} + \eta_2(s_{25} - s_{24}/\mu_2) \\ A_{32} &= s_{41}\mu_2 + s_{42}/\mu_2 - s_{46} + \eta_2(s_{45} - s_{44}/\mu_2) \\ A_{13} &= \eta_3(s_{11}\mu_3^2 + s_{12} - s_{16}\mu_3) + s_{15}\mu_3 - s_{14} \\ A_{23} &= \eta_3(s_{21}\mu_3 + s_{22}/\mu_3 - s_{26}) + s_{25} - s_{24}/\mu_3 \\ A_{33} &= \eta_3(s_{41}\mu_3 + s_{42}/\mu_3 - s_{46}) + s_{45} - s_{44}/\mu_3 \end{aligned}$$

and

$$\begin{aligned} \eta_1 &= -l_3(\mu_1)/l_2(\mu_1) \\ \eta_2 &= -l_3(\mu_2)/l_2(\mu_2) \\ \eta_3 &= -l_3(\mu_3)/l_4(\mu_3) \end{aligned}$$

Hereafter, the boldface is used to represent a vector or a matrix throughout this paper unless stated otherwise.

2.1. Singularities in a homogeneous medium

Consider a homogeneous medium subjected to a dislocation line, with Burger's vector $\boldsymbol{b}$ and a line force $\boldsymbol{p}$, in the direction perpendicular to $x_1 - x_2$ plane. The stress function of the isolated singularity at the point (x_{D1}, x_{D2}) in an infinite homogeneous medium is (Eshelby et al., 1953)

$$\boldsymbol{f}_0(z) = \boldsymbol{q}\ln(z - z^{\mathrm{D}}), \quad z_\alpha^{\mathrm{D}} = x_{D1} + \mu_\alpha x_{D2} \tag{10}$$

The complex coefficient vector $\boldsymbol{q}$ is defined as

$$\boldsymbol{q} = \frac{1}{2\pi}\left(\boldsymbol{L}^{-1}(\boldsymbol{B} + \overline{\boldsymbol{B}})^{-1}\boldsymbol{b} - \boldsymbol{A}(\boldsymbol{B}^{-1})^{-1}\boldsymbol{p}\right) \tag{11}$$

where $\boldsymbol{b} = \boldsymbol{u}^+ - \boldsymbol{u}^-$, $\boldsymbol{p} = \boldsymbol{t}^- - \boldsymbol{t}^+$ and $\boldsymbol{B} = \mathrm{i}\boldsymbol{A}\boldsymbol{L}^{-1}$.

Next, consider a crack of length 2a lying along the x_1-axis subjected to an arbitrary self-equilibrated traction $\boldsymbol{t}_{\mathrm{s}}(x_1)$ prescribed on its surfaces. This crack problem leads to a Hilbert problem and the singular stress function can be expressed as (Muskhelishvili, 1953)

$$\boldsymbol{L}\boldsymbol{f}'_0(z) = \frac{\chi(z)}{2\pi i}\int_{-a}^{a}\frac{\boldsymbol{t}_{\mathrm{s}}(\xi)\,\mathrm{d}\xi}{\chi(\xi)(\xi - z)} \tag{12}$$

where the plemelj function $\chi(z)$ is defined as

$$\chi(z) = (z - a)^{-\frac{1}{2}}(z + a)^{-\frac{1}{2}} \tag{13}$$

For the problem with various crack orientations, a new coordinate system is defined such that its origin is translated to the central point of the crack (x_{c1}, x_{c2}) and then rotated by an angle θ with respect to x_1-axis, as shown Fig. 1. The singular stress function of this new coordinate system can be determined by using the coordinate transformation, which is expressed as (Ting, 1986)

$$\boldsymbol{L}^*\boldsymbol{f}'^*_0(z^*) = \frac{\chi^*(z^*)}{2\pi i}\int_{-a}^{a}\frac{\boldsymbol{t}^*_{\mathrm{s}}(\xi)\,\mathrm{d}\xi}{\chi^*(\xi)(\xi - z^*)} \tag{14}$$

where the superscript * denotes the variable with respect to the new coordinate. The formula of coordinate transformation can be shown as

$$x_i^* = R_{ij}(x_j - x_{cj}), \quad i = j = 1, 2, 3 \tag{15}$$

Note that x_i^* and x_j represent the new and old coordinate system, respectively and x_{cj} denotes the origin of the new coordinate system with respect to the old coordinate system. Then, the coordinate rotation coefficient can be expressed as

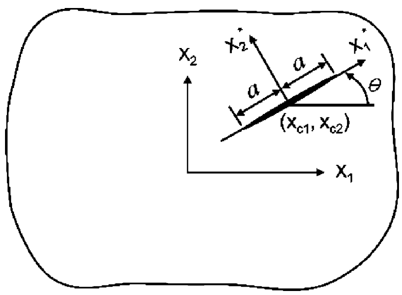

Fig. 1. Oblique crack coordinate system.

$$\boldsymbol{R} = \{R_{ij}\} = \left[\frac{\partial x_i^*}{\partial x_j}\right] = \begin{bmatrix} \cos\theta & \sin\theta & 0 \\ -\sin\theta & \cos\theta & 0 \\ 0 & 0 & 1 \end{bmatrix} \tag{16}$$

The complex variable z^* in the new coordinate system is defined as

$$z_\alpha^* = x_1^* + \mu_\alpha x_2^* \quad (\alpha = 1,2,3) \tag{17}$$

with $\boldsymbol{L}^* = \boldsymbol{RL}$, $\boldsymbol{A}^* = \boldsymbol{RA}$, $\mu_\alpha^* = \frac{\mu_\alpha \cos\theta - \sin\theta}{\mu_\alpha \sin\theta + \cos\theta}$, $\alpha = 1,2,3$.

The asymptotic solution to the crack tip is of interest for the crack problem. The conventional definition of stress intensity factors is given by (Irwin, 1957)

$$\boldsymbol{K} = [K_{\mathrm{II}} \quad K_{\mathrm{I}} \quad K_{\mathrm{III}}]^{\mathrm{T}} = \lim_{r\to 0} \sqrt{2\pi r}\,\boldsymbol{t}^* \tag{18}$$

where $r = x_1^* - a$ denotes the radius ahead the crack tip at $x_1^* = a$, and

$$\boldsymbol{t}^* = 2\Re\{\boldsymbol{L}^* \boldsymbol{f}_0'^*(z^*)\} \tag{19}$$

which represents the traction along x_1^*-axis. Substituting Eq. (19) into Eq. (18) with the aid of Eq. (14), the stress intensity factor can be expressed as

$$\boldsymbol{K} = \frac{-1}{\sqrt{\pi a}} \int_{-a}^{a} \sqrt{\frac{a+\xi}{a-\xi}}\, \boldsymbol{t}_s^*(\xi)\, \mathrm{d}\xi \tag{20}$$

From Eq. (20), the traction prescribed on the crack surface needs to be determined before solving the asymptotic solution of the crack tip.

2.2. Singularities in a bimaterial

The solution of singularities in a bimaterial problem can be directly obtained from the substitution of the solution to that associated with an infinite homogeneous medium by using the technique of analytical continuation. If the singularities, and $\boldsymbol{f}_0(z)$ for the same singularities embedded in an infinite homogeneous medium, are taken to be in the upper half space of the bimaterial (see Fig. 2), then the solution can be assumed as

$$\boldsymbol{f}(z) = \begin{cases} \boldsymbol{f}_a(z) + \boldsymbol{f}_0(z) & z \in a \\ \boldsymbol{f}_b(z) & z \in b \end{cases} \tag{21}$$

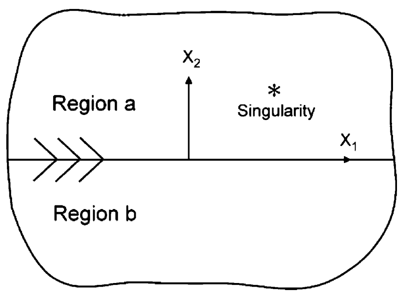

Fig. 2. A singularity in a bimaterial.

where $\boldsymbol{f}_a(z)$ and $\boldsymbol{f}_b(z)$ are the corresponding analytic functions in the upper half space (region a) and lower half space (region b), respectively. Assume that the bonding of interface is perfect, then the traction (or resultant force) and displacement across the interface must be continuous. From Eq. (7), it requires that

$$\begin{aligned} \boldsymbol{L}_a[\boldsymbol{f}_a(x_1)+\boldsymbol{f}_0(x_1)]+\overline{\boldsymbol{L}}_a[\bar{\boldsymbol{f}}_a(x_1)+\bar{\boldsymbol{f}}_0(x_1)] &= \overline{\boldsymbol{L}}_b\bar{\boldsymbol{f}}_b(x_1)+\boldsymbol{L}_b\boldsymbol{f}_b(x_1) \\ \boldsymbol{A}_a[\boldsymbol{f}_a(x_1)+\boldsymbol{f}_0(x_1)]+\overline{\boldsymbol{A}}_a[\bar{\boldsymbol{f}}_a(x_1)+\bar{\boldsymbol{f}}_0(x_1)] &= \overline{\boldsymbol{A}}_b\bar{\boldsymbol{f}}_b(x_1)+\boldsymbol{A}_b\boldsymbol{f}_b(x_1) \end{aligned} \tag{22}$$

where the suffix a and b indicate the material properties of upper (a) and lower (b) half space, respectively. One of the important properties of analytical (holomorphic) functions used in the method of analytical continuous is that if $\varphi(z)$ is analytical in an upper half space (or a lower half space), then $\overline{\varphi(\bar{z})}$ is analytical in a lower half space (or an upper half space). Use of the method of analytical continuation and application of Eq. (22) leads to

$$\begin{cases} \boldsymbol{f}_a(z) = \overline{\boldsymbol{V}}_{ba}\bar{\boldsymbol{f}}_0(z) & z\in a \\ \boldsymbol{f}_b(z) = \boldsymbol{U}_{ba}\boldsymbol{f}_0(z) & z\in b \end{cases} \tag{23}$$

where

$$\boldsymbol{V}_{ba} = \overline{\boldsymbol{L}}_a^{-1}(\boldsymbol{B}_b+\overline{\boldsymbol{B}}_a)^{-1}(\boldsymbol{B}_a-\boldsymbol{B}_b)\boldsymbol{L}_a$$

$$\boldsymbol{U}_{ba} = \boldsymbol{L}_b^{-1}[\boldsymbol{I}+(\boldsymbol{B}_b+\overline{\boldsymbol{B}}_a)^{-1}(\boldsymbol{B}_a-\boldsymbol{B}_b)]\boldsymbol{L}_a$$

with $\boldsymbol{B}_a = \mathrm{i}\boldsymbol{A}_a\boldsymbol{L}_a^{-1}$, $\boldsymbol{B}_b = \mathrm{i}\boldsymbol{A}_b\boldsymbol{L}_b^{-1}$.

Substitution of Eq. (23) into Eq. (22) gives the complete solution to a bimaterial subjected to singularities in the upper half space. If a bimaterial is subjected to singularities in the lower half space, the solution can be assumed as

$$\boldsymbol{f}(z) = \begin{cases} \boldsymbol{f}_a(z) & z\in a \\ \boldsymbol{f}_b(z)+\boldsymbol{f}_0(z) & z\in b \end{cases} \tag{24}$$

and one finds, by the similar procedure,

$$\begin{cases} \boldsymbol{f}_a(z) = \boldsymbol{U}_{ab}\boldsymbol{f}_0(z) & z\in a \\ \boldsymbol{f}_b(z) = \overline{\boldsymbol{V}}_{ab}\bar{\boldsymbol{f}}_0(z) & z\in b \end{cases} \tag{25}$$

2.3. Singularities in a bimaterial with the interface at $x_2 = h$

Assume that regions a and b occupied with material a and b, are perfectly bonded along the interface $x_2 = h$. With $x_1 - x_2$ coordinate system lying off the interface, it needs to reformulate the bimaterial solution obtained in the previous section. The solution is also assumed as Eq. (21), in which $\boldsymbol{f}_a(z)$ and $\boldsymbol{f}_b(z)$ are introduced to satisfy the continuity of tractions and displacements along the interface $x_2 = h$. By applying the same arguments used in Eq. (22) to the interface $x_2 = h$, one finds

$$\begin{cases} \boldsymbol{f}_a(z) = \overline{\boldsymbol{V}}_{ba}\bar{\boldsymbol{f}}_0(z-\mu_a h+\bar{\mu}_a h) & z\in a \\ \boldsymbol{f}_b(z) = \boldsymbol{U}_{ba}\boldsymbol{f}_0(z-\mu_b h+\mu_a h) & z\in b \end{cases} \tag{26}$$

Substitution of Eq. (26) into (21) gives the complete solution to a bimaterial subjected to singularities in the upper half space. If a bimaterial with the interface at $x_2 = h$ is subjected to singularities in the lower half space, $\boldsymbol{f}_a(z)$ and $\boldsymbol{f}_b(z)$ are obtained as

$$\begin{cases} \boldsymbol{f}_a(z) = \boldsymbol{U}_{ab}\boldsymbol{f}_0(z-\mu_a h+\mu_b h) & z\in a \\ \boldsymbol{f}_b(z) = \overline{\boldsymbol{V}}_{ab}\bar{\boldsymbol{f}}_0(z-\mu_b h+\bar{\mu}_b h) & z\in b \end{cases} \tag{27}$$

Substitution of Eq. (27) into (24) gives the complete solution to a bimaterial subjected to singularities in the lower half space.

2.4. Singularities in a trimaterial with the interfaces at $x_2 = 0$ and $x_2 = h$

The alternating technique can be employed to analyze a singularity in a trimaterial with two parallel interfaces at $x_2 = 0$ and $x_2 = h$ (see Fig. 3). Since it is difficult to satisfy the continuity conditions along two interfaces at the same time, the method of analytic continuation should be applied to two interfaces alternatively.

Assume that regions a, b and c occupied with material a, b and c, respectively are perfectly bonded along the interfaces $x_2 = 0$ and $x_2 = h$ (see Fig. 3). Consider that a trimaterial is subjected to singularities in region b, the alternating technique is applied to solve the complete solution by considering the following steps.

First, we consider that regions a and b are composed of the same material b and region c of material c. As in Eq. (21), if $\boldsymbol{f}_0(z)$ is taken to be a homogeneous solution and $\boldsymbol{f}_1(z)$ and $\boldsymbol{f}_{c0}(z)$ are introduced to satisfy the continuity of displacements and tractions across the interface $x_2 = 0$, Eq. (23) leads to

$$\begin{cases} \boldsymbol{f}_1(z) = \overline{\boldsymbol{V}}_{cb}\bar{\boldsymbol{f}}_0(z) + \boldsymbol{f}_0(z) & z \in a \cup b \\ \boldsymbol{f}_{c0}(z) = \boldsymbol{U}_{cb}\boldsymbol{f}_0(z) & z \in c \end{cases} \tag{28}$$

Since this result is based on the assumption that region a is made up of material b. The fields produced by $\boldsymbol{f}_1(z)$ cannot satisfy the continuity conditions at the interface $x_2 = h$, which lies between the material a and b.

In the second step, regions b and c are composed of the same material b and region a of material a. $\boldsymbol{f}_1(z)$ in Eq. (28) having the singular points in region $b \cup c$ is treated as a homogeneous solution of material b. $\boldsymbol{f}_{a1}(z)$ and $\boldsymbol{f}_{b1}(z)$ are introduced to satisfy the continuity of displacements and tractions across the interface $x_2 = h$, Eq. (27) leads to

$$\begin{cases} \boldsymbol{f}_{a1}(z) = \boldsymbol{U}_{ab}\boldsymbol{f}_1(z - \mu_a h + \mu_b h) & z \in a \\ \boldsymbol{f}_{b1}(z) = \overline{\boldsymbol{V}}_{ab}\bar{\boldsymbol{f}}_1(z - \mu_b h + \bar{\mu}_b h) & z \in b \cup c \end{cases} \tag{29}$$

in which $\boldsymbol{f}_{a1}(z)$ and $\boldsymbol{f}_{b1}(z)$ can be expressed in term of $\boldsymbol{f}_0(z)$ through Eq. (28). Here $\bar{\boldsymbol{f}}_i(z - \mu_a h + \bar{\mu}_a h) = \overline{\boldsymbol{f}_i(\bar{z} - \bar{\mu}_a h + \mu_a h)}$. Since this result is based on the assumption that region c is made up of material b. The fields produced by $\boldsymbol{f}_{b1}(z)$ cannot satisfy the continuity conditions at the interface $x_2 = 0$, which lies between the material b and c.

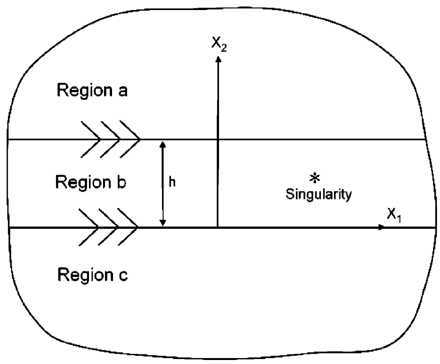

Fig. 3. A singularity in a trimaterial.

In the third step, regions a and b are composed of the same material b and region c of material c. $\boldsymbol{f}_{b1}(z)$ in Eq. (29) having the singular points in region $a \cup b$ is treated as a homogeneous solution of material b. $\boldsymbol{f}_2(z)$ and $\boldsymbol{f}_{c1}(z)$ are introduced to satisfy the continuity of displacements and tractions across the interface $x_2 = 0$. Accordingly it can be shown from Eq. (23) that

$$\begin{cases} \boldsymbol{f}_2(z) = \overline{\boldsymbol{V}}_{cb}\bar{\boldsymbol{f}}_{b1}(z) & z \in a \cup b \\ \boldsymbol{f}_{c1}(z) = \boldsymbol{U}_{cb}\boldsymbol{f}_{b1}(z) & z \in c \end{cases} \tag{30}$$

Since this result is based on the assumption that region a is made up of material b. The fields produced by $\boldsymbol{f}_2(z)$ cannot satisfy the continuity conditions at the interface $x_2 = h$, which lies between the material a and b.

In the fourth step, regions b and c are composed of the same material b and region a of material a. Repetitions of second and third step, the stress functions at the regions a, b and c can be finally obtained as

$$\boldsymbol{f}(z) = \begin{cases} \boldsymbol{f}_{a1}(z) + \boldsymbol{f}_{a2}(z) + \cdots & z \in a \\ \boldsymbol{f}_1(z) + \boldsymbol{f}_{b1}(z) + \boldsymbol{f}_2(z) + \boldsymbol{f}_{b2}(z) \cdots & z \in b \\ \boldsymbol{f}_{c0}(z) + \boldsymbol{f}_{c1}(z) + \boldsymbol{f}_{c2}(z) \cdots & z \in c \end{cases} \tag{31}$$

If one expresses the stress functions in terms of $\boldsymbol{f}_0(z)$, Eq. (31) becomes

$$\boldsymbol{f}(z) = \begin{cases} \boldsymbol{U}_{ab} \sum_{n=1}^{\infty} \boldsymbol{f}_n(z - \mu_a h + \mu_b h) & z \in a \\ \sum_{n=1}^{\infty} \left[\boldsymbol{f}_n(z) + \overline{\boldsymbol{V}}_{ab}\bar{\boldsymbol{f}}_n(z - \mu_b h + \bar{\mu}_b h)\right] & z \in b \\ \boldsymbol{U}_{cb}\boldsymbol{f}_0(z) + \boldsymbol{U}_{cb}\overline{\boldsymbol{V}}_{ab} \sum_{n=1}^{\infty} \left[\bar{\boldsymbol{f}}_n(z - \mu_b h + \bar{\mu}_b h)\right] & z \in c \end{cases} \tag{32}$$

in which the recurrence formula for $\boldsymbol{f}_n(z)$ is

$$\boldsymbol{f}_{n+1}(z) = \begin{cases} \boldsymbol{f}_0(z) + \overline{\boldsymbol{V}}_{cb}\bar{\boldsymbol{f}}_0(z) & n = 0 \\ \overline{\boldsymbol{V}}_{cb}\boldsymbol{V}_{ab}\boldsymbol{f}_n(z - \bar{\mu}_b h + \mu_b h) & n = 1, 2, 3, \ldots \end{cases} \tag{33}$$

3. Formulation of viscoelasticity

For a linear viscoelastic material, the strain or stress at any given time is the sum of the individual strain or stress increments through the respective time intervals during which they have been applied. By Boltzman's superposition principle, the relationship between strain and stress can be written in the hereditary integral (Christensen, 1982),

$$\varepsilon_{ij}(t) = \int_{-\infty}^{t} s_{ijkl}(t - \xi)\,\mathrm{d}\sigma_{kl}(\xi) \tag{34}$$

where s_{ijkl} is known as creep compliance which can be obtained by the creep test. Eq. (34) can also be written as

$$\varepsilon_{ij}(t) = s_{ijkl}(0)\sigma_{kl}(t) + \int_0^t s'_{ijkl}(t - \xi)\sigma_{kl}(\xi)\,\mathrm{d}\xi \tag{35}$$

for $t \geqslant 0$ and $i, j, k = 1, 2, 3$, or in contracted form

$$\varepsilon_m(t) = s_{mn}(0)\sigma_n(t) + \int_0^t s'_{mn}(t - \xi)\sigma_n(\xi)\,\mathrm{d}\xi \tag{36}$$

where $m, n = 1, 2, \ldots, 6$.

Consider that any function $g(t)$ and define the Laplace transform of $g(t)$ as

$$\hat{g}(p) = \int_0^\infty g(t)\mathrm{e}^{-pt}\,\mathrm{d}t \tag{37}$$

where p denotes the Laplace transform parameter. Taking the Laplace transform of Eq. (36), the strain–stress relationship becomes

$$\hat{\varepsilon}_m(p) = \hat{s}_{mn}(p)\hat{\sigma}_n(p) \tag{38}$$

With the definition of Eq. (37), the viscoelastic field corresponding to Eq. (7) can be written as

$$\begin{aligned} \hat{\boldsymbol{u}} &= \hat{\boldsymbol{A}}\hat{\boldsymbol{f}}(\hat{z}) + \overline{\hat{\boldsymbol{A}}\hat{\boldsymbol{f}}(\hat{z})} \\ \hat{\boldsymbol{t}} &= \widehat{\boldsymbol{L}}\hat{\boldsymbol{f}}'(\hat{z}) + \overline{\widehat{\boldsymbol{L}}\hat{\boldsymbol{f}}'(\hat{z})} \end{aligned} \tag{39}$$

where all coefficients in the Eq. (39) can be obtained by a simple alternation from the previous definition, for example

$$\hat{z}_\alpha = x_1 + \hat{\mu}_\alpha x_2 \quad (\alpha = 1, 2, 3) \tag{40}$$

and

$$\hat{l}_2(\hat{\mu})\hat{l}_4(\hat{\mu}) - \hat{l}_3^2(\hat{\mu}) = 0 \tag{41}$$

where

$$\begin{aligned} \hat{l}_2(\hat{\mu}) &= \hat{s}_{44} - 2\hat{s}_{45}\hat{\mu} + \hat{s}_{55}\hat{\mu}^2 \\ \hat{l}_3(\hat{\mu}) &= -\hat{s}_{24} + (\hat{s}_{25} + \hat{s}_{46})\hat{\mu} - (\hat{s}_{14} + \hat{s}_{56})\hat{\mu}^2 + \hat{s}_{15}\hat{\mu}^3 \\ \hat{l}_4(\hat{\mu}) &= \hat{s}_{22} - 2\hat{s}_{26}\hat{\mu} + (2\hat{s}_{12} + \hat{s}_{66})\hat{\mu}^2 - 2\hat{s}_{16}\hat{\mu}^3 + \hat{s}_{11}\hat{\mu}^4 \end{aligned} \tag{42}$$

It is easily shown that the only difference between the viscoelastic and elastic representations is that $\hat{s}_{mn}$ appears in the viscoelastic set whereas s_{mn} appears in the elastic set. Taking the Laplace transform of the viscoelastic set produces a set of equations which correspond in a one-to-one fashion to the elastic set. This is called a correspondence principle (Christensen, 1982, 1984).

Referring to Fig. 4, consider a thin cracked layer (region b) bonded to a viscoelastic substrate (region c) under an arbitrary concentrated force (***P***). By letting region a be non-existent, the problem of a trimaterial subjected to singularities in region b is now reduced to the present problem of a thin cracked layer bonded to a viscoelastic substrate under an arbitrary concentrated force. From the previous definition, the Laplace transformed stress intensity factor is given as

$$\widehat{K} = \lim_{r\to 0}\sqrt{2\pi r}\,\hat{\boldsymbol{t}}^* \tag{43}$$

where

$$\hat{\boldsymbol{t}}^* = 2\Re\left\{\widehat{\boldsymbol{L}}_b^*\hat{\boldsymbol{f}}'_b(\hat{z})\right\} \tag{44}$$

with

$$\hat{\boldsymbol{f}}'_b(\hat{z}) = \sum_{n=1}^{\infty}\left[\hat{\boldsymbol{f}}'_n(\hat{z}) + \hat{\overline{\boldsymbol{V}}}_{ab}\hat{\overline{\boldsymbol{f}}}'_n(\hat{z} - \hat{\mu}_b h + \hat{\bar{\mu}}_b h)\right] \tag{45}$$

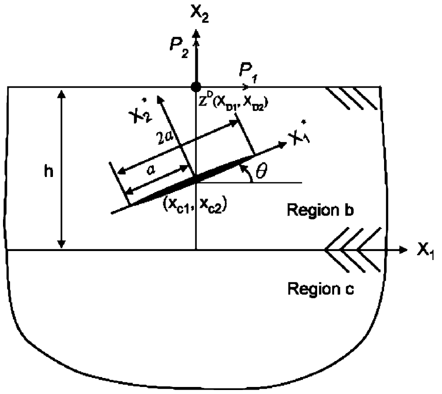

Fig. 4. A crack embedded in the thin layer medium with a half space substrate.

in which the recurrence formula for $\hat{\boldsymbol{f}}'_n(\hat{z})$ is

$$\hat{\boldsymbol{f}}'_{n+1}(\hat{z}) = \begin{cases} \hat{\boldsymbol{f}}'_0(\hat{z}) + \widehat{\overline{\boldsymbol{V}}}_{cb}\hat{\overline{\boldsymbol{f}}}'_0(\hat{z}) & n = 0 \\ \widehat{\overline{\boldsymbol{V}}}_{cb}\widehat{\boldsymbol{V}}_{ab}\hat{\boldsymbol{f}}'_n(\hat{z} - \hat{\bar{\mu}}_b h + \hat{\mu}_b h) & n = 1, 2, 3, \ldots \end{cases} \tag{46}$$

Note that the 3×3 matrices $\widehat{\boldsymbol{V}}_{ab}$ and $\widehat{\boldsymbol{V}}_{cb}$ in Eqs. (45) and (46) are now defined as

$$\widehat{\boldsymbol{V}}_{ab} = -\widehat{\overline{\boldsymbol{L}}}_b^{-1}\widehat{\boldsymbol{L}}_b$$

$$\widehat{\boldsymbol{V}}_{cb} = \widehat{\overline{\boldsymbol{L}}}_b^{-1}(\widehat{\boldsymbol{B}}_c + \widehat{\overline{\boldsymbol{B}}}_b)^{-1}(\widehat{\boldsymbol{B}}_b - \widehat{\boldsymbol{B}}_c)\widehat{\boldsymbol{L}}_b$$

Then, the real time stress intensity factor can be directly obtained by taking the inverse Laplace transform of Eq. (43).

4. Numerical results

Applying the standard solid model to simulate the viscoelastic property, the constitutive equation in Eq. (36) can be expressed as

$$\varepsilon_m(t) = s^0_{mn}\left\{\sigma_n(t) + \eta\int_0^t f(t-\xi)\sigma_n(\xi)\,\mathrm{d}\xi\right\} \tag{47}$$

and

$$\eta = \frac{(s^\infty_{mn} - s^0_{mn})}{s^0_{mn}\lambda}, \quad f(t) = \mathrm{e}^{-t/\lambda} \tag{48}$$

where λ indicates the relaxation constant, s^0_{mn} and s^∞_{mn} denote the creep compliance at $t = 0$ and time-elapse, respectively. In the following discussion, we consider an elastic cracked layer made of the cortical bone (region b) bonded to a viscoelastic substrate made of the cancellous bone (region c) subjected to a concentrated force (see Fig. 4). The material properties of the cortical bone and the cancellous bone are listed in Table 1. Consider a transversely isotropic material, the elements of the compliance tensor can be expressed as (Leknitskii, 1963)

Table 1
Material properties of a thin layer medium and a half space substrate

	E_1 (MPa)	E_2 (MPa)	v_{12}	v_{23}	G_{12} (MPa)
Thin layer (Cortical bone)	20×10^3	18.7×10^3	0.24	0.29	4.6×10^3
Substrate (Cancellous bone)	1×10^3	0.8×10^3	0.315	0.35	0.24×10^3
			$\lambda=\eta=1$		

$$s_{11}=\frac{E_1-v_{12}^2E_2}{E_1^2},\quad s_{22}=\frac{1-v_{23}^2}{E_2},\quad s_{12}=s_{21}=-\frac{v_{12}(1+v_{23})}{E_1},\\ s_{44}=\frac{2(1+v_{23})}{E_2},\quad s_{55}=s_{66}=\frac{1}{G_{12}} \tag{49}$$

where all other elements vanish. Note that the relationship in Eq. (49) can also apply to the viscoelastic properties of the substrate if one replaces s_{mn} in Eq. (49) with s_{mn}^0.

In view of Eq. (20), Eq. (43) can be written as

$$\widehat{\boldsymbol{K}}=\lim_{r\to 0}\sqrt{2\pi r}\hat{\boldsymbol{t}}^*=\frac{-1}{\sqrt{\pi a}}\int_{-a}^{a}\sqrt{\frac{a+\xi}{a-\xi}}\hat{\boldsymbol{t}}_p^*(\xi,p)\,\mathrm{d}\xi \tag{50}$$

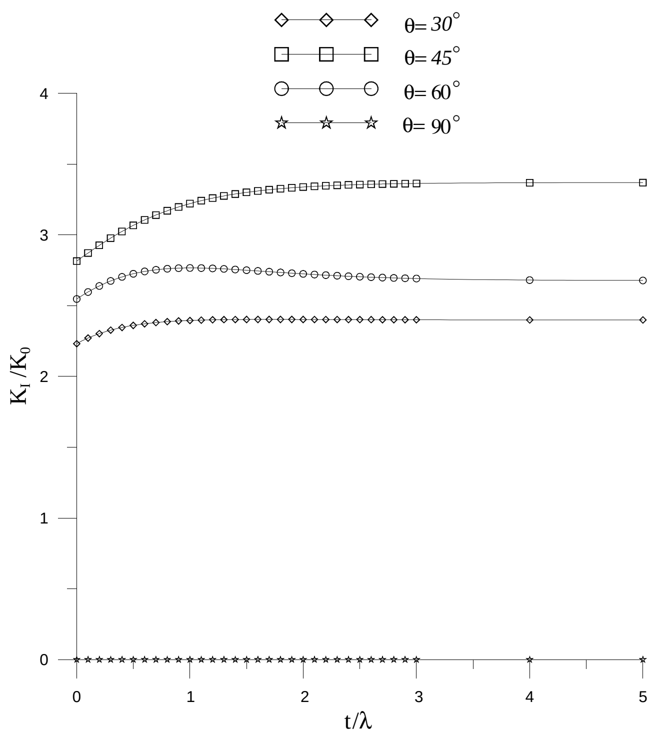

Fig. 5. Mode-I stress intensity factor (K_{I}) for various crack orientations subjected to a horizontal concentrated force ($\boldsymbol{P}=[-P_1,0]$) with $a/h=0.25$.

where $\hat{\boldsymbol{t}}_p^*(\xi, p)$ can be derived from Eqs. (44)–(46). Then, the real-time stress intensity factor becomes

$$\boldsymbol{K}(t) = \frac{-1}{\sqrt{\pi a}} \int_{-a}^{a} \sqrt{\frac{a+\xi}{a-\xi}} \boldsymbol{t}_p^*(\xi, t)\, \mathrm{d}\xi \tag{51}$$

where $\boldsymbol{t}_p^*(\xi, t)$ is the inverse Laplace transform of $\hat{\boldsymbol{t}}_p^*(\xi, p)$. For a linear viscoelastic problem, $\boldsymbol{t}_p^*(\xi, t)$ can be found numerically by the direct inverse method (Christensen, 1982, 1962, 1996). However, the inverse transform of the present complex equations is not easily treated using the direct inverse method. Hence, the Mathematica software (Wolfram Research, USA) is used to solve the inverse Laplace transform in this study. Having the function $\boldsymbol{t}_p^*(\xi, t)$ at hand, the stress intensity factor in Eq. (51) can be obtained numerically by dividing the integral path into $2n$ segments as

$$\begin{aligned} \boldsymbol{K}(t) &= \frac{-1}{\sqrt{\pi a}} \int_{-a}^{a} \sqrt{\frac{a+\xi}{a-\xi}} \boldsymbol{t}_p^*(\xi, t)\, \mathrm{d}\xi = \frac{-1}{\sqrt{\pi a}} \sum_{i=-n}^{n-1} \int_{\frac{ai}{n}}^{\frac{a(i+1)}{n}} \sqrt{\frac{a+\xi}{a-\xi}} \boldsymbol{t}_p^*(\xi_i, t)\, \mathrm{d}\xi_i \\ &\cong \frac{-1}{\sqrt{\pi a}} \sum_{i=-n}^{n-1} t_p^*\left(\frac{ai}{n} + h_s, t\right) \int_{\frac{ai}{n}}^{\frac{a(i+1)}{n}} \sqrt{\frac{a+\xi_i}{a-\xi_i}} \mathrm{d}\xi_i \\ &\cong \frac{-1}{\sqrt{\pi a}} \sum_{i=-n}^{n-1} \boldsymbol{t}_p^*\left(\frac{ai}{n} + h_s, t\right) \left[a \cdot \mathrm{Arc}\sin\left(\frac{\xi_i}{a}\right) - \sqrt{a^2 - \xi_i^2}\right]_{\xi_i = \frac{ai}{n}}^{\xi_i = \frac{a(i+1)}{n}} \end{aligned} \tag{52}$$

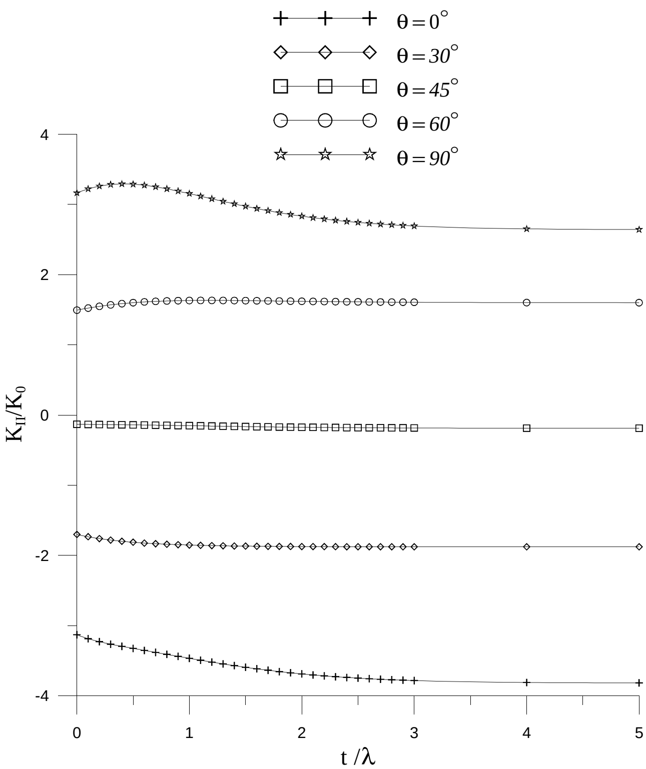

Fig. 6. Mode-II stress intensity factor (K_{II}) for various crack orientations subjected to a horizontal concentrated force ($\boldsymbol{P} = [-P_1, 0]$) with $a/h = 0.25$.

since $\boldsymbol{t}_p^*(\xi,t)$ is continuous along the integral path $-a < \xi < a$ and the integral $\int_{-a}^{a}\sqrt{a+\xi/a-\xi}\,d\xi$ exists. In Eq. (52), h_s denotes any arbitrary point within each segment, i.e. $0 \leqslant h_s \leqslant a/n$. It will show that the numerical method in Eq. (52) produces a very good convergence in the following discussion for $n \geqslant 100$.

The main interest here is to analyze the bone defect where a crack is embedded in the cortical bone bonded to the cancellous bone having a viscoelastic property. In the following discussion, the center of the crack with length $a/h = 0.25$ is fixed at $x_{c1} = 0$, $x_{c2} = 0.5h$ and the concentrated force is located at $x_{D1} = 0$, $x_{D2} = h$ (see Fig. 4). All the calculated results are, which are presented only at the right crack tip, evaluated with terms up to $n = 4$ in Eq. (32). The normalized stress intensity factors K_{I} and K_{II} versus the evolution of time under a negative horizontal concentrated force ($\boldsymbol{P} = [-P_1, 0]$) with the dimensionless factor $K_0 = P_1/2\sqrt{\pi a}$ are shown in Figs. 5 and 6, respectively. For a given crack angle, as shown in Fig. 5, the K_{I} value converges to its long-time value as time elapses. This convergent value is treated as the elastic response. It shows that the K_{I} value increases with time until it approaches a long-time constant value for the crack angle $\theta = 30°$, $\theta = 45°$ and $\theta = 60°$ while the K_{I} value almost remains constant as time elapses for the crack angle $\theta = 90°$. It is clear that the effect of cancellous bone is less significant for the stress intensity factor K_{I} when a crack is placed parallel or normal to the free surface under a horizontal concentrated force. It also exhibits that, for various crack angles, the maximum K_{I} value occurs at $\theta = 45°$ and the minimum K_{I} value at $\theta = 0°$. In contrast with the variation of K_{I} in the case of the horizontal loading, the effect of cancellous bone is more significant for the stress intensity factor K_{II} when a crack is placed parallel ($\theta = 0°$) or normal ($\theta = 90°$) to the free surface. In addition, the maximum K_{II} value occurs at $\theta = 0°$ and the minimum occurs at $\theta = 45°$. The normalized stress intensity factors K_{I} and K_{II} versus the evolution of

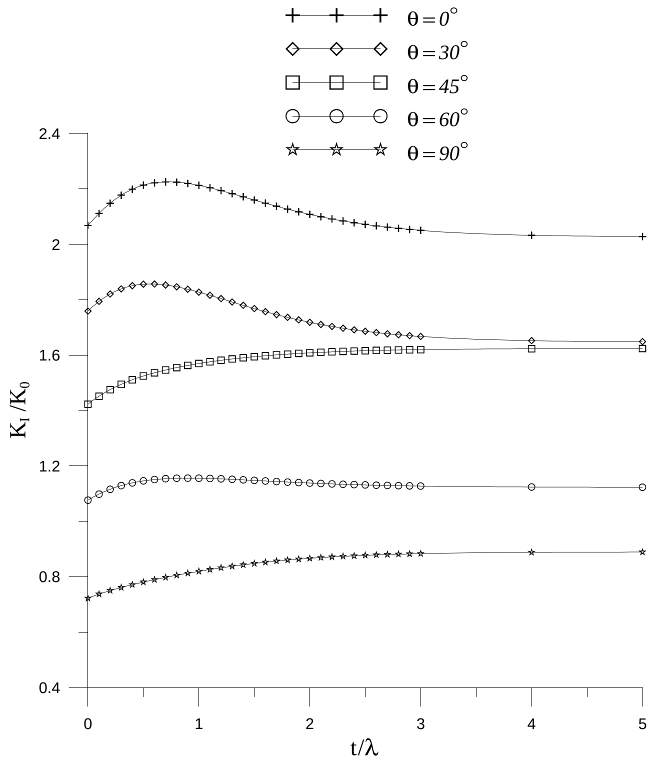

Fig. 7. Mode-I stress intensity factor (K_{I}) for various crack orientations subjected to a vertical concentrated force ($\boldsymbol{P} = [0, P_2]$) with $a/h = 0.25$.

time under a vertical concentrated force ($\boldsymbol{P} = [0, P_2]$) are shown in Figs. 7 and 8, respectively. Fig. 7 shows that, for a given crack angle $\theta = 0°$, $\theta = 30°$ or $\theta = 60°$, the normalized K_{I} increases with time, reaches a maximum value at a particular time and decreases with time until it approaches a long-time constant value. This implies that K_{I} has a maximum value during the evolution of time or the change of the substrate strength. For various crack orientations, the maximum K_{I} value occurs at $\theta = 0°$ and the minimum value occurs at $\theta = 90°$. When the long-time value is considered, the maximum K_{I} value still occurs at $\theta = 0°$. The normalized K_{II} values are shown in Fig. 8, which remain nearly unchanged during the evolution of time for the crack angle $\theta = 0°$ and $\theta = 90°$. It means that the effect of cancellous bone is less significant for the stress intensity factor K_{II} when a crack is placed parallel or normal to the free surface under a vertical concentrated force. As in the case of K_{I}, where the maximum value occurred at $\theta = 45°$ under a horizontal concentrated force, the maximum K_{II} value is found to occur at $\theta = 45°$ under a vertical concentrated force.

In order to demonstrate the accuracy and convergence of our present derived solutions, we consider the following two testing examples. First, we consider a dislocation in a Ge_xSi_{1-x} epilayer on a Si substrate. The elastic constants of Ge, Si, and Ge_xSi_{1-x} with respect to the crystallographic axes, where x represents the fraction of lattice sites occupied by Ge atoms, are given in Table 2 (Zhang, 1995). The image force in x_2 direction per unit length of a dislocation in material b due to two parallel interfaces in a trimaterial is given by

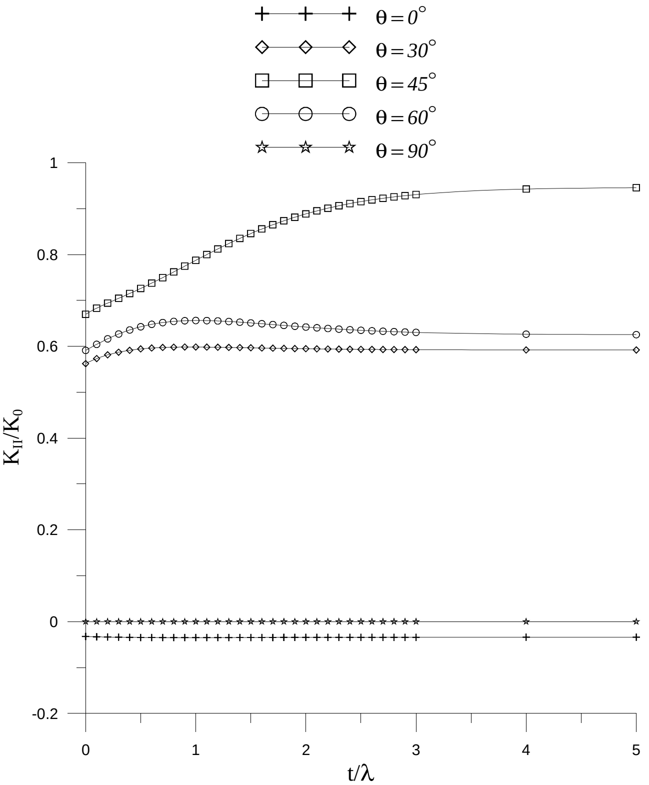

Fig. 8. Mode-II stress intensity factor (K_{II}) for various crack orientations subjected to a vertical point force ($\boldsymbol{P} = [0, P_2]$) with $a/h = 0.25$.

Table 2
Elastic constants of Ge, Si, and Ge_xSi_{1-x} in unit of GPa (Zhang, 1995) with respect to crystallographic directions

Crystal	c_{11}	c_{12}	c_{44}
Ge	128.9	48.3	67.1
Si	165.7	63.9	79.6
Ge_xSi_{1-x}	$128.9x + 165.7(1-x)$	$48.3x + 63.9(1-x)$	$67.1x + 79.6(1-x)$

$$f_2 = 2\boldsymbol{b}Re\left\{\boldsymbol{L}_b\langle\boldsymbol{\mu}_b\rangle\left[\overline{\boldsymbol{V}}_{cb}\bar{\boldsymbol{f}}'_0(s) + \sum_{n=2}^{\infty}\boldsymbol{f}'_n(s) + \overline{\boldsymbol{V}}_{ab}\sum_{n=1}^{\infty}\bar{\boldsymbol{f}}'_n(s - \mu_b h + \bar{\mu}_b h)\right]\right\} \tag{53}$$

Fig. 9 displays the image force f_2/f_{free} exerted on the 60° dislocation for $x = 0.1$, 0.3 and 0.5 with $\{1\,0\,0\}$ plane epitaxy. The normalizing constant f_{free} is the image force on the dislocation at a distance h from $\{1\,0\,0\}$ free surface in Si half space. The results in Fig. 9, which are evaluated with terms up to $n = 3$ in Eq. (32), agree very well with the Fig. 4 of Choi and Earmme (2002a).

Next, we consider a crack of length $2a$ embedded in an elastic isotropic homogeneous medium subjected to a point force P acting on its surface. The exact solution for stress intensity factors at the right-hand tip are given as (Sih et al., 1962)

$$\frac{K_{\text{I}}}{K_a} = \frac{1-v}{2(1+v)} \quad \frac{K_{\text{II}}}{K_a} = \sqrt{\frac{1 + x_a/a}{1 - x_a/a}} \tag{54}$$

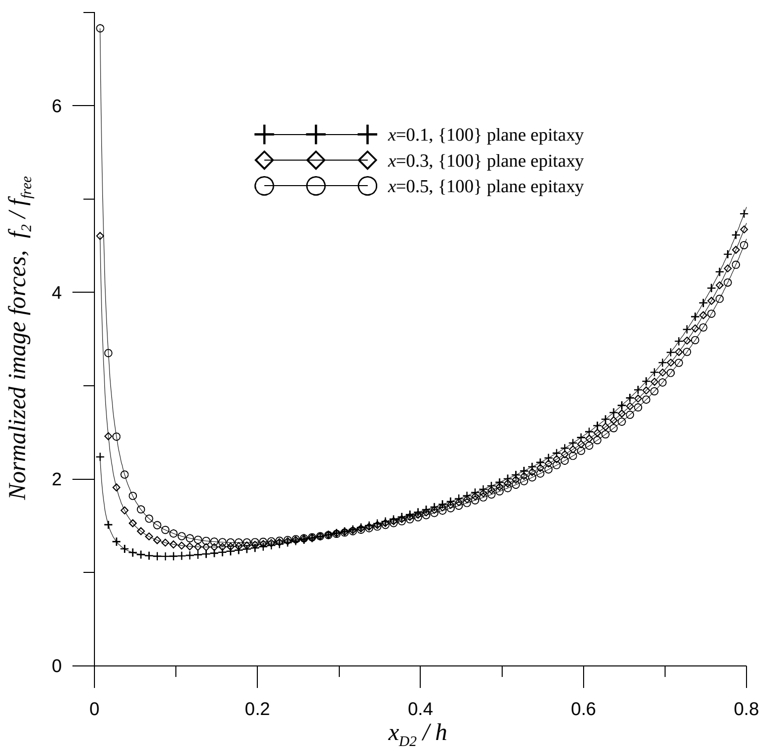

Fig. 9. Normalized image forces versus the position of a dislocation.

Table 3
Stress intensity factors for a vertical point force acting on the crack surface with $v = 0.335$

$\frac{x_a}{a}$	K_I/K_a			K_{II}/K_a		
	Theoretical value	Numerical value	Error %	Theoretical value	Numerical value	Error %
0	1.000	1.000	<0.1	−0.249	−0.246	1.3
0.1	1.106	1.106	<0.1	−0.249	−0.246	1.3
0.2	1.225	1.225	<0.1	−0.249	−0.246	1.3
0.3	1.363	1.363	<0.1	−0.249	−0.246	1.3
0.4	1.578	1.528	<0.1	−0.249	−0.246	1.4
0.5	1.732	1.732	<0.1	−0.249	−0.246	1.4
0.6	2.000	2.000	<0.1	−0.249	−0.245	1.5
0.7	2.380	2.380	<0.1	−0.249	−0.245	1.6
0.8	3.000	3.000	<0.1	−0.249	−0.244	2.0
0.9	4.359	4.359	<0.1	−0.249	−0.240	3.4

Table 4
Stress intensity factors for a horizontal point force acting on the crack surface with $v = 0.335$

$\frac{x_a}{a}$	K_I/K_a			K_{II}/K_a		
	Theoretical value	Numerical value	Error %	Theoretical value	Numerical value	Error %
0	0.249	0.250	0.3	1.000	1.000	<0.1
0.1	0.249	0.250	0.3	1.106	1.106	<0.1
0.2	0.249	0.250	0.3	1.225	1.225	<0.1
0.3	0.249	0.250	0.3	1.363	1.363	<0.1
0.4	0.249	0.250	0.2	1.578	1.528	<0.1
0.5	0.249	0.249	0.2	1.732	1.732	<0.1
0.6	0.249	0.249	0.1	2.000	2.000	<0.1
0.7	0.249	0.249	0.1	2.380	2.380	<0.1
0.8	0.249	0.248	0.4	3.000	3.000	<0.1
0.9	0.249	0.244	1.9	4.359	4.359	<0.1

for a horizontal point force and

$$\frac{K_I}{K_a} = \sqrt{\frac{1 + x_a/a}{1 - x_a/a}} \quad \frac{K_{II}}{K_a} = -\frac{1 - v}{2(1 + v)} \tag{55}$$

for a vertical point force, where $K_a = P/2\sqrt{\pi a}$ and x_a indicates the distance between the crack center and the position of the point force P. Comparisons of the theoretical value and the present numerical long-time value for the crack surface subjected a vertical and a horizontal point force are shown in Tables 3 and 4, respectively. These results show that the numerical values of the present study are found to agree very well with the analytical solution.

5. Conclusion

Based on the alternating technique and the method of analytical continuation, the solution to the problem with singularities in an anisotropic trimaterial is provided in this study. The trimaterial solution obtained here can be directly applied to the present problem with a thin layer bonded to a half-plane substrate. With this fundamental solution, the stress intensity factors for the corresponding crack problem are determined by solving the singular integral equation. Based on a correspondence principle, the real-time stress intensity factors for the corresponding viscoelastic problem can be obtained by taking the inverse Laplace transform. Some typical examples, including various loading types and crack orientations, are solved and discussed in detail. The results show that the effect of substrate is more (or less) significant for the stress intensity factor K_{II} (or K_I) when the crack is placed parallel or normal to the free surface under a horizontal concentrated force. In addition, the maximum K_I (or K_{II}) value is found to occur at $\theta = 45°$ in the case of a horizontal (or vertical) loading. The obtained results are useful in studying the problem with a crack embedded in the cortical bone that is bonded to the cancellous bone having a viscoelastic property.

Acknowledgement

The authors would like to thank the support by the National Science Council, Republic of China, through grant no. NSC 91-2212-E-011-032.

References

Atkinson, C., Bourne, J.P., 1989. Stress singularities in viscoelastic media. Quart. J. Mech. Appl. Math. 42, 385–412.
Atkinson, C., Chen, C.Y., 1996. The influence of layer thickness on the stress intensity factor of a crack lying in an elastic (viscoelastic) layer embedded in a different elastic (viscoelastic) medium (mode III analysis). Int. J. Eng. Sci. 34, 639–658.
Chang, R.C., 2002. On the general treatment of a cracked multi-layered medium in antiplane viscoelasticity. Mech. Mater. 34, 61–71.
Chang, R.C., Wang, S.C., Chao, C.K., 2001. Effects of a viscoelastic substrate on a cracked body under in-plane concentrated loading. Acta Mech. 148, 215–229.
Chao, C.K., Kao, B., 1997. A thin cracked layer bonded to an elastic half-space under an antiplane concentrated load. Int. J. Fract. 83, 223–241.
Choi, S.T., Earmme, Y.Y., 2002a. Elastic study on singularities interacting with interfaces using alternating technique: Part I. Anisotropic trimaterial. Int. J. Solids Struct. 39, 943–957.
Choi, S.T., Earmme, Y.Y., 2002b. Elastic study on singularities interacting with interfaces using alternating technique: Part II. Isotropic trimaterial. Int. J. Solids Struct. 39, 1199–1211.
Christensen, R.M., 1982. Theory of Viscoelasticity. An Introduction, second ed. Academic Press, New York.
Eshelby, J.D., Read, W.T., Shockley, W., 1953. Anisotropic elasticity with applications to dislocation theory. Acta Metall. 1, 251–259.
Irwin, G.R., 1957. Analysis of stress and strain near the end of a crack transversing a plate. J. Appl. Mech. 24, 109–114.
Leknitskii, S.G., 1963. Theory of an Anisotropic Elastic Body. Holden-Day, San Francisco.
Miller, G.R., 1989. Analysis of cracks near interfaces between dissimilar anisotropic materials. Int. J. Eng. Sci. 27, 667–678.
Muskhelishvili, N.I., 1953. Some Basic Problems of Mathematical Theory of Elasticity. Noor-doff, Groningen.
Ryvkin, M., Banks-Sills, L., 1993. Steady-state mode III propagation of an interface crack in an inhomogeneous viscoelastic strip. Int. J. Solids Struct. 30, 483–498.
Ryvkin, M., Banks-Sills, L., 1994. Mode III delamination of a viscoelastic strip from a dissimilar viscoelastic half-plane. Int. J. Solids Struct. 31, 551–566.
Schapery, R.A., 1962. Approximate method of transform inversion for viscoelastic stress analysis. In: Proceedings of the 4th US National Congress of Applied Mechanics, pp. 1075–1086.
Schapery, R.A., 1984. Correspondence principles and a generalized J integral for large deformation and fracture analysis of viscoelastic media. Int. J. Fract. 25, 195–223.
Sih, G.C., Paris, P.C., Erdogan, F., 1962. Crack tip, stress-intensity factor for plane extension and plane bending problem. J. Appl. Mech. 29, 306–312.
Stroh, A.N., 1958. Dislocation and cracks in anisotropic elasticity. Philos. Mag. 7, 625–646.
Suo, Z., 1990. Singularities, interfaces and cracks in dissimilar anisotropic media. Proc. Roy. Soc. London, Ser. A 427, 331–358.
Ting, T.C.T., 1986. Explicit solution and invariance of the singularities at an interface crack in anisotropic composites. Int. J. Solids Struct. 22, 956–983.
Zhang, T.Y., 1995. Anisotropic elasticity study of the critical thickness of an epilayer on a substrate with different elastic constants. J. Appl. Mech. 78, 4948–4957.